

Probing the Supersymmetric Standard Model at the LHC through Vector Boson Fusion and Machine Learning

Umar Qureshi¹ Alfredo Gurrola¹

¹Department of Physics and Astronomy, Vanderbilt University, Nashville, TN, USA

16th International Workshop on Boosted Object Phenomenology, Reconstruction, Measurements, and Searches at Colliders

July 31st 2024



Table of Contents

- 1 Introduction and Motivation
- 2 Proposed Analysis Strategy
- 3 Simulating Signal and Background Events
- 4 Analysis using Machine Learning
- 5 Discussion and Conclusion

Motivation: The Incompleteness of the Standard Model

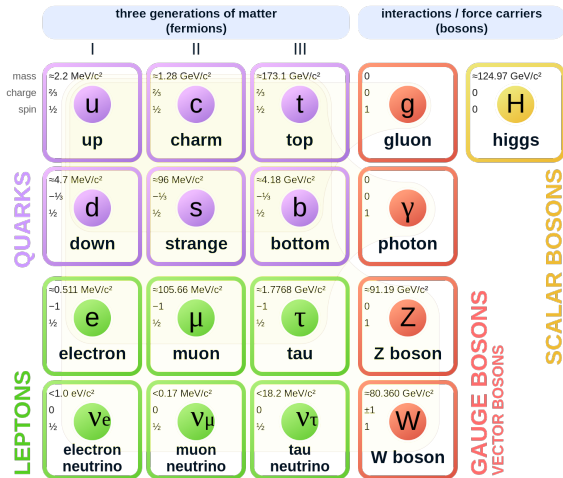


Figure 1: The Standard Model of Particle Physics.

The Standard Model

The Standard Model (SM) of particle physics is a successful theory describing:

- Three of the four fundamental forces.
- All observed elementary matter particles.

Incompleteness of the SM

However, it fails to account for:

- Dark Matter and Dark Energy.
- Higgs Mass.
- The Gauge Hierarchy Problem.
- Neutrino Masses.
- A plethora of experimental anomalies.

Introducing Supersymmetry

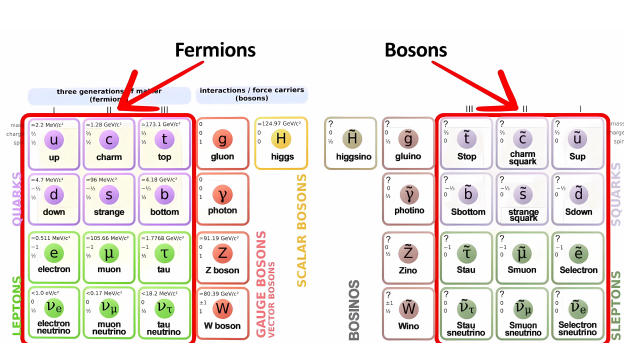


Figure 2: A Supersymmetric Standard Model.

Supersymmetry (SUSY):

Restores symmetry between fermions and bosons.

Supersymmetric Particles

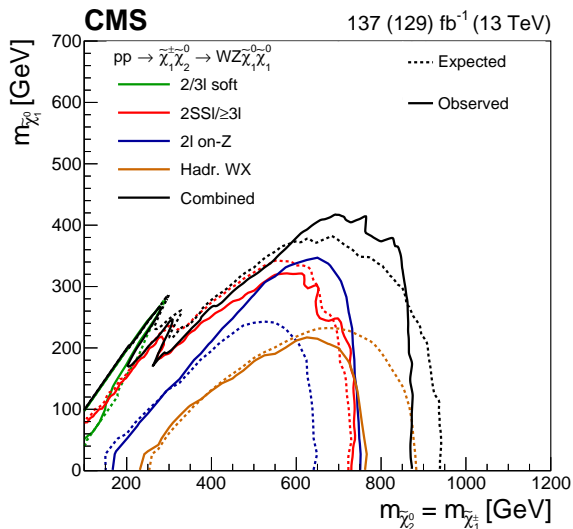
- New *superpartners* of SM particles.
- Spins of partner SUSY and SM particles differ by 1/2.

Theoretical Motivations

SUSY models can simultaneously address:

- Dark matter (DM).
- The Hierarchy Problem.
- Higgs Mass.
- Neutrino Masses.*
- Several anomalies.

Experimental Constrains on SUSY



Experimental Constraints

Bounds on the colored SUSY sector exclude at the 95% CL:

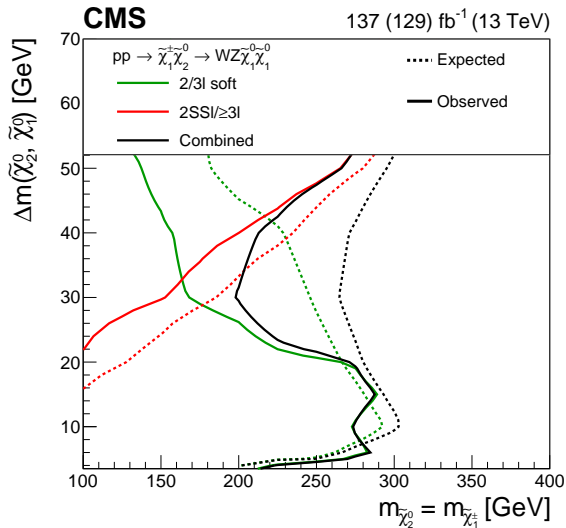
- Gluinos \tilde{g} up to 2.31 TeV.
- Stops \tilde{t} up to 1.25 TeV
- Sbottoms \tilde{b} up to 1.24 TeV.

Bounds on the electroweak sector are more relaxed, excluding:

- Charginos $\tilde{\chi}_1^\pm$ and second-gen neutralinos $\tilde{\chi}_2^0$ up to 950 GeV.
- First-gen neutralinos $\tilde{\chi}_1^0$ up to 400 GeV.

Figure 3: SUS-21-008: Bino-wino Exclusion Contours.

Compressed Mass Spectrum Scenarios



Compressed Mass Spectrum

- $m(\tilde{\chi}_1^\pm) = m(\tilde{\chi}_2^0)$.
- $\Delta m(\tilde{\chi}_2^0, \tilde{\chi}_1^0)$ is small.
- Soft SM decay products.
- Traditionally challenging, bounds are lower.
- VBF and ML can help.

- For this talk, we fix $\Delta m = 50$.

Figure 4: SUS-21-008: Compressed-Mass Contours.

Traditional SUSY Electroweakino Searches

Electroweakino Pair Production

Traditional SUSY searches consider:

- Electroweakino Drell-Yan-like pair production.
- Typically no associated particles/jets.

Final States

- Typically a mix of hadronic or leptonic.
- Decay products of $V/V^*/H$.

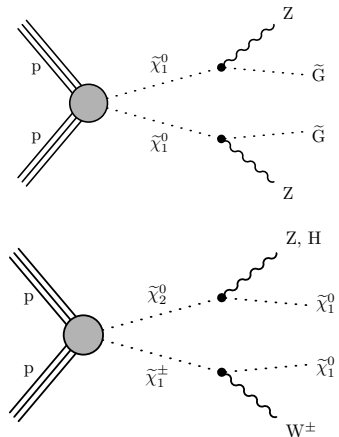


Figure 5: Representative Feynman Diagrams for $\tilde{\chi}_1^0\tilde{\chi}_1^0$ (top) and $\tilde{\chi}_2^0\tilde{\chi}_1^\pm$ (bottom) pair production and subsequent decay.

Vector Boson Fusion (VBF)

The VBF Topology

- Quarks from protons radiate vector bosons.
- These bosons fuse to produce a particle.
- The quarks are minimally deflected.
- Leading to jets in the forward direction.

VBF Jet Signature

- VBF jets have large mass.
- Found in opposite hemispheres.

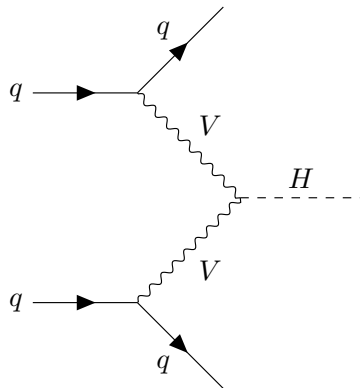


Figure 6: Representative Feynman Diagram for VBF Higgs Production.

Our Proposed Analysis Strategy

The Model

- We probe the Minimal Supersymmetric SM.
- R-parity is conserved.
- The LSP $\tilde{\chi}_1^0$ is purely bino.
- The NLSPs $\tilde{\chi}_1^\pm$ and $\tilde{\chi}_2^0$ are purely wino and mass-degenerate.
- The sleptons ($\tilde{e}, \tilde{\mu}, \tilde{\tau}$) are left-handed, mass-degenerate, and heavier than the $\tilde{\chi}_1^\pm$ and $\tilde{\chi}_{1,2}^0$.

Signal Process

Our signal is the pure electroweak VBF process:

$$pp \rightarrow \text{ewkino ewkino } jj$$

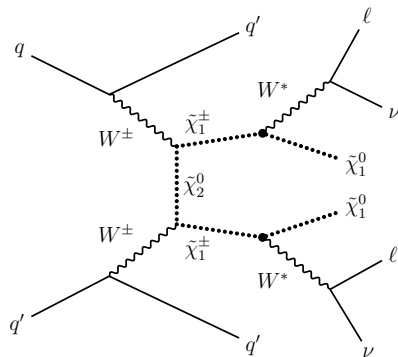


Figure 7: Representative Feynman diagram for VBF chargino-chargino pair production, and subsequent decay to a 2-lepton final state.

Our Proposed Analysis Strategy

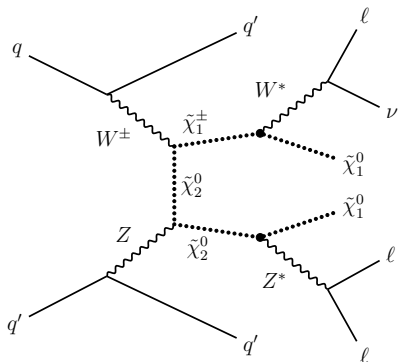


Figure 8: Representative Feynman diagram for VBF chargino-neutralino pair production and subsequent decay to a 3-lepton final state.

Decay Mode

Due to the high slepton masses, the branching fraction ratios are:

$$\mathcal{B}(\tilde{\chi}_1^\pm \rightarrow \tilde{\chi}_1^0 W^{\pm,*}) = 1$$

$$\mathcal{B}(\tilde{\chi}_2^0 \rightarrow \tilde{\chi}_1^0 Z^*) = 1$$

Final States

- Large MET from neutrinos and $\tilde{\chi}_1^0$.
- VBF-tagged dijets.
- 0, 1, 2, 3, or 4 leptons.

Event Selection Criteria

- $\geq 1\ell$ with $p_T > 5$ GeV and $|\eta| < 2.5$.
- $p_T(j) > 20$ GeV and $|\eta(j)| < 5$.

Background Determination

The most important backgrounds are:

- $pp \rightarrow V + \text{Jets}$.
- $pp \rightarrow VVjj$.
- $pp \rightarrow t\bar{t}$.

Several others were considered:

- QCD multijets.
- Triboson.

But were not relevant ($\ll 1\%$ effect).

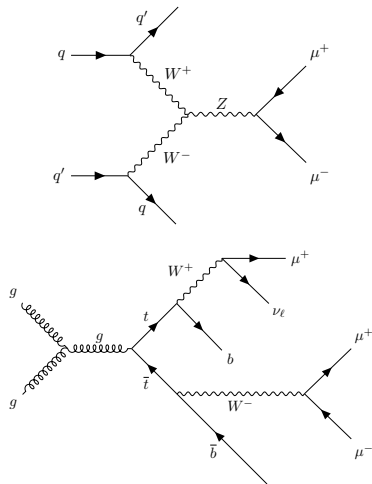


Figure 9: Representative Feynman diagrams for VBF dilepton with two jets (top) and $t\bar{t}$ with semi-leptonic decay (bottom).

Simulating Signal and Background Events

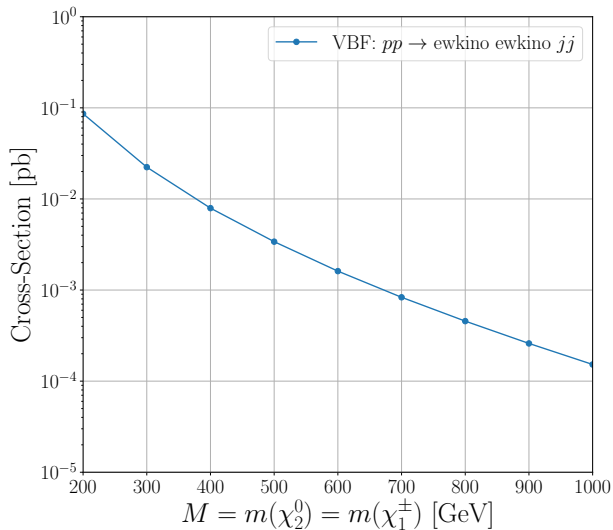


Figure 10: Signal cross-section vs. $\tilde{\chi}_2^0$ and $\tilde{\chi}_1^\pm$ masses.

Signal and Background Simulation

Samples $n = 10^7$ are produced using:

- MadGraph5 for event generation.
- Pythia8 for parton showering and hadronization.
- Delphes for detector effects.

- The SUSY colored sector is decoupled.
- Generator-level cuts of $\Delta\eta(jj) > 3.5$ and $m(jj) > 200$ GeV are imposed.

Event Kinematic Distribution Analysis

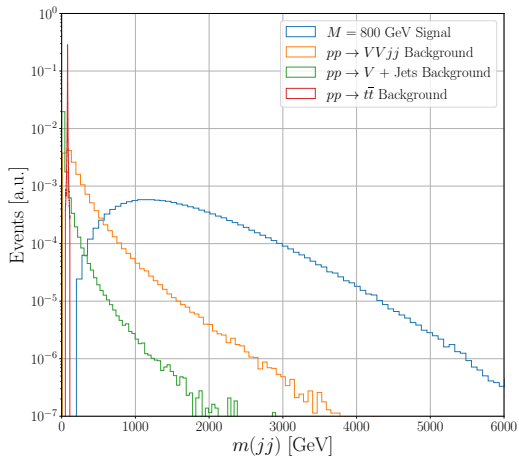


Figure 11: Dijet Invariant Mass Distribution.

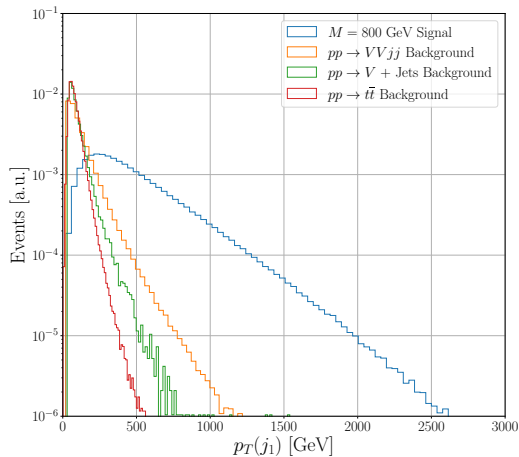


Figure 12: Leading Jet p_T Distribution.

Event Kinematic Distribution Analysis

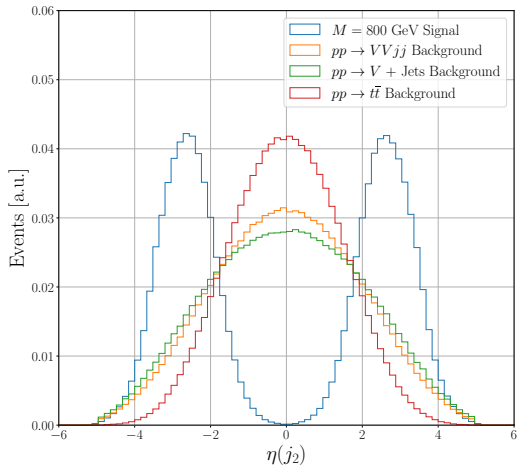


Figure 13: Subleading Jet η Distribution.

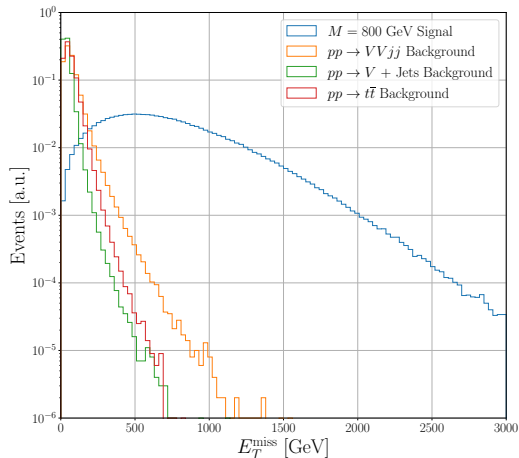


Figure 14: Missing E_T Distribution.

Analysis using Machine Learning (ML)

ML Advantages

- Simultaneous fit to all variables.
- Thus, yields greater sensitivity.

Signal-Background Discrimination

- Use event kinematics as features.
- Combine signal-background events.
- Use ML for signal-background discrimination.

ML Model Details

Boosted decision tree with parameters:

- $\eta = 0.6$, $\gamma = 0$, `max_depth = 6`.

Implemented using XGBoost.

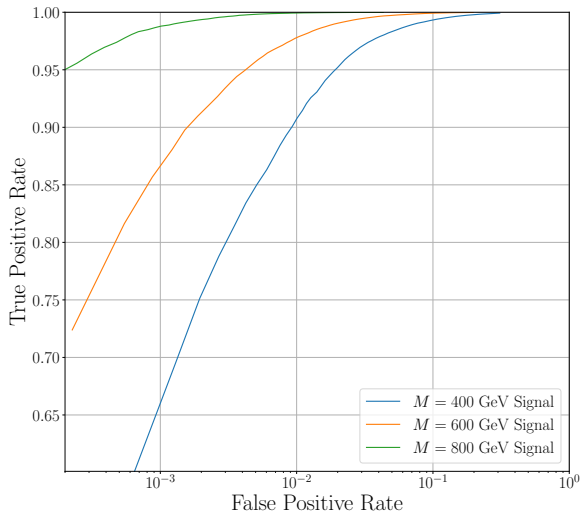


Figure 15: ROC Curves for the BDT.

Signal Significance

The BDT outputs are normalized to:

$$N = \mathcal{L}_{\text{int}} \cdot \sigma \cdot \varepsilon$$

A bin-by-bin calculation is used to compute signal significance:

$$SS = \frac{\sum s_i w_i}{\sqrt{\sum (s_i + b_i) w_i^2 + \beta^2 \sum w_i^2 (s_i^2 + b_i^2)}}$$

Where s_i , b_i are the number of signal and background events in the i^{th} bin, β is the systematic uncertainty, and w_i is:

$$w_i = \ln \left(1 + \frac{s_i}{b_i} \right)$$

Selection and Detector Efficiencies

- Jet efficiency is $> 95\%$.
- Lepton efficiency is $\approx 90\%$.
- Taken into account as ε factor.

Uncertainties

A flat 15% systematic uncertainty β :

- 3% on the CMS measurement of \mathcal{L}_{int} .
- 5% in jet energy scale uncertainties.
- 2% in the BDT distribution shape.
- 10% in the signal and background predictions.

Results: Signal Significance

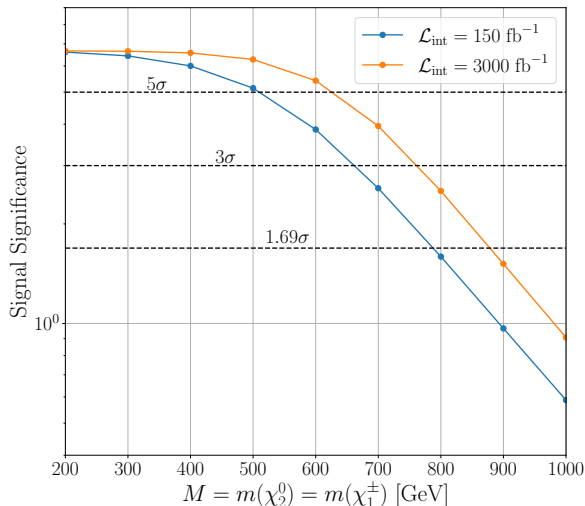


Figure 16: Signal Significance vs. $\tilde{\chi}_2^0$ and $\tilde{\chi}_1^\pm$ masses.

Extending LHC Constrains to SUSY

Constraints to $\tilde{\chi}_2^0$ and $\tilde{\chi}_1^\pm$ masses at a:

- $\geq 5\sigma$ signal significance for masses up to **660 (520) GeV**.
- $\geq 3\sigma$ signal significance for masses up to **770 (620) GeV**.
- $\geq 95\%$ confidence level for masses up to **880 (750) GeV**.

Integrated luminosities of 3000 (150) fb^{-1} .

Conclusion

- We extend LHC constraints to $\tilde{\chi}_1^\pm$ and $\tilde{\chi}_{1,2}^0$ by over 4 times in the compressed-mass spectrum region using VBF production and ML.

Future Work

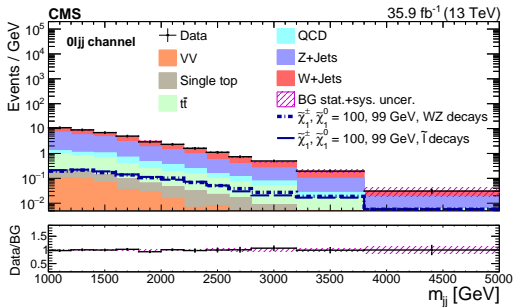
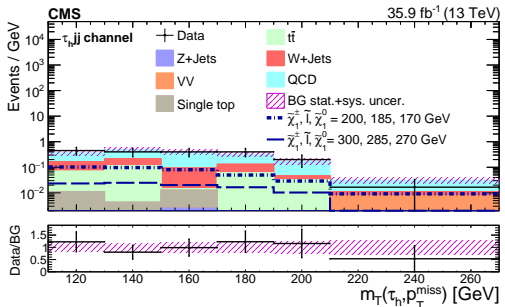
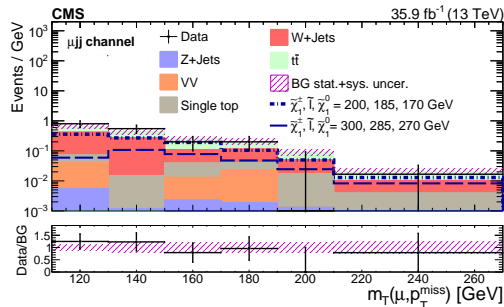
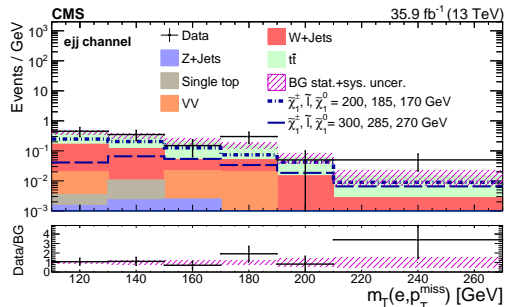
- Extend the parameter space for various Δm values $\in [5, 75]$ GeV.
- Newer ML models? Generative models to learn features directly from data/simulation?
- Currently, we are also performing a full experimental search at CMS using this methodology.

Acknowledgements

- I thank Professor Alfredo Gurrola for his invaluable support and guidance.
- This work is supported in part by NSF Award PHY-1945366 and a Vanderbilt Seeding Success Grant.

Thank you! Questions?

Appendix: CMS-SUS-21-008 Observed $m(jj)$ and m_T Distributions



Appendix: Event Composition Ratio

Process	$\tilde{\chi}_1^\pm \tilde{\chi}_2^0$	$\tilde{\chi}_1^\pm \tilde{\chi}_1^0$	$\tilde{\chi}_1^\pm \tilde{\chi}_1^\pm$	$\tilde{\chi}_2^0 \tilde{\chi}_2^0$	$\tilde{\chi}_2^0 \tilde{\chi}_1^0$	$\tilde{\chi}_1^0 \tilde{\chi}_1^0$
Composition [%]	30.5	< 0.1	54.7	14.8	< 0.1	< 0.1

Table 1: Event composition ratio for different electroweakino pair combinations included in the signal processes for a benchmark $M = 100$ GeV signal with $\Delta m = 5$.